2015 International Symposium on Nonlinear Theory and its Applications
NOLTA2015, Kowloon, Hong Kong, China, December 1-4, 2015

Linear local modes produced by an intrinsic local mode in a saturable nonlinear lattice

S. Shige†, W. Shi†, T. Ishikawa†, T. Nakaguchi†, M. Sato† and A. J. Sievers‡

†Graduate School of Natural Science and Technology, Kanazawa University
Kakumamachi, Kanazawa, Ishikawa 920-1192, Japan
‡Laboratory of Atomic and Solid State Physics, Cornell University
Ithaca, NY 14853-2501, USA
Email: temde@stu.kanazawa-u.ac.jp, msato153@staff.kanazawa-u.ac.jp

Abstract– An electrical transmission line array composed from FETs as nonlinear saturable elements is studied. As a function of the driving frequency the saturable nonlinearity causes the intrinsic local mode (ILM) width to change in a stepwise manner. At the step transition the mode symmetry changes between odd and even. Linear local modes associated with the ILM are observed to change in number as a step is crossed.

1. Introduction

In a nonlinear lattice, a stationary stable localized excitation called an intrinsic localized mode (ILM) or discrete breather (DB) can be generated due to discreteness. [1-4] Progress has been made to produce traveling ILMs free from lattice pinning. [5-12] Introducing a saturable nonlinearity into the lattice is one such method. [13-17] With increase in ILM energy saturation of the nonlinearity increases the spatial width of the ILM. This is to be contrasted with the usual nonlinear case, which gives rise to a narrower ILM width with increasing energy. When the ILM width widens at a transition step, the symmetry of the ILM changes from even (odd) to odd (even), and the stability of odd and even modes are interchanged. At this transition point, both even and odd modes have the same stability, and this equality assists the lateral translational movement of the ILM. We have already reported the interchange of stability between even and odd symmetry ILMs by experimentally observing the frequencies of these modes in a nonlinear lattice containing MOS-FET's as the saturable nonlinear capacitor. [18]

In this paper, we demonstrate that in addition to a linear local mode (LLM) nearby the ILM frequency, [19] other more distant LLMs exist when the ILM saturable nonlinearity is very large. By experimentally counting the number of LLMs associated with the ILM on either side of a width transition it is discovered that the number changes by one when the width transition is crossed.

2. Experiment

Figure 1(a) shows a schematic of the circuit set up, which produces the saturable nonlinear lattice. It is similar to the design used previously, [18] except for the saturable capacitor. In this study, the drain terminal of the FET is opened, causing a larger nonlinearity and a larger hysteresis at the transition. The measured saturable capacitance vs voltage is shown in Fig. 1(b). Only a slight difference is observed between up and down scanning curves, probably due to some carriers remaining at the open drain terminal when the FET is turned off. This may be the cause of the large hysteresis at the step transitions. The linear dispersion curve for this transmission line is shown in Fig. 1(c). Because of the soft nonlinearity, the ILM frequency appears below the bottom of the dispersion curve.

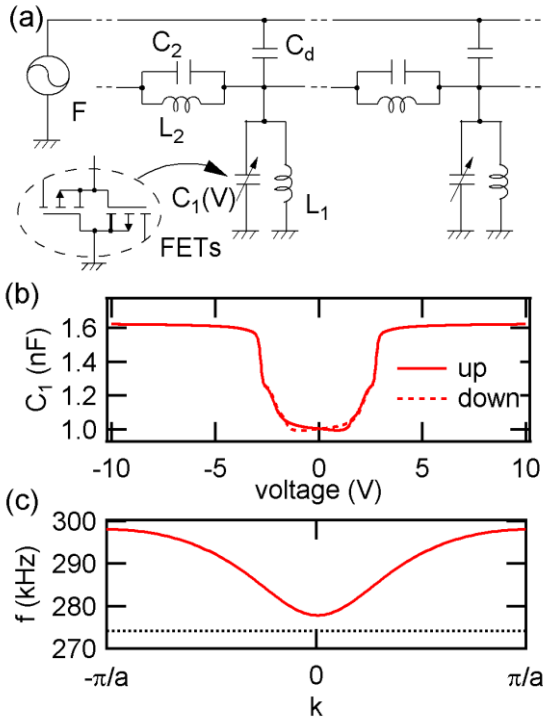

Fig. 1. (a) Circuit diagram of the saturable nonlinear lattice. Lattice size is 16. Two FETs are connected anti-parallel and used as a saturable capacitor. (b) Capacitance as a function of the bias voltage. (c) Linear dispersion curve. Dotted line indicates typical pump frequency.

Two oscillators are used in the measurements, one is called the pump and has a large ac voltage while the other, the probe, has a very small voltage. The pump is used to generate and maintain the ILM in steady state. The ILM is generated by lowering the pump frequency, *F*, starting from the bottom of the dispersion curve. The resulting amplitude pattern is changed by incrementally shifting the pump frequency. The probe is used to measure the resulting linear response spectrum for each pump increment. The probe frequency *f* is scanned across the pump frequency *F*, and the response caused by the probe is recorded. Since the probe voltage is small the ILM state, maintained by the large amplitude pump, is unchanged during the probe scan.

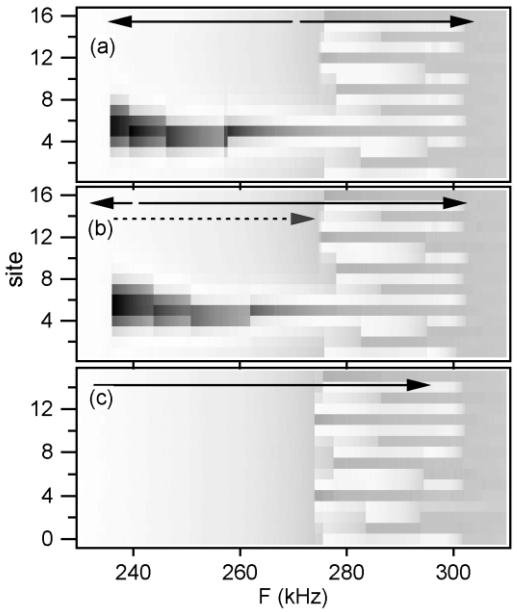

Fig. 2 Spatial pattern of the ILM in the saturable nonlinear lattice vs pump frequency. Arrows indicate direction of pump frequency change. (a) Frequency is varying up and down from middle of the figure. (b) Frequency is increased with the ILM present. Dashed arrow indicates the frequency direction for the linear response measurement. (c) Scan from low frequency where no ILM is observed.

3. Experimental Results

Figure 2 shows ILM patterns in real space as a function of the pump frequency, *F*. A darker pattern means larger oscillation amplitude. Solid arrows in Figs. 2(a)-(c) identify pump frequency scanning directions. (The pattern above 275kHz in (a-c) is due to an acoustic band excitation with a wavy modulation.) Figure 2(a) indicates that the ILM centered around site 5 becomes broader in a step-wise manner as the pump frequency is decreased. Hysteresis in the step frequency with scan direction can be seen by comparing step positions between Figs. 2(a) and (b). Note the very large hysteresis between Figs. 2(a) and (c).

Figure 3 presents the linear response spectra obtained by scanning the pump frequency according to the dashed arrow in Fig. 2(b). The pump frequency *F* is given along the right side. The large peak at negative $(f-F)$ values is the natural oscillator frequency (NF), which softens as the ILM becomes unstable, $(f-F)\to 0$. [20] At the top of this figure, the NF peak is very close to $(f-F)=0$, and gradually shifts left as pump frequency *F* increases from top to bottom. The other NF peak at the symmetric position to $(f-F)=0$ is hard to see in this case. It is only barely visible in the frequency region *F*=263~274kHz, and identified by arrow NF*. Other peaks observed on the positive side of the figure have been identified with LLMs and band modes from the bottom of the dispersion curve. The series of peaks farthest to the right are such band modes. Three peaks for F= 234 KHz identified by the arrows are LLMs associated with the ILM. They appear when the ILM nonlinearity is very strong.

The three step transitions observed in Fig. 2(b) are found to produce sudden changes in the linear response curves in Fig. 3. They can be seen at around 244, 251 and 262kHz. Approaching the 244kHz transition from 234 KHz, the 1st LLM softens and disappears, so that only two LLMs remain. Since it is the closest LLM in frequency to the ILM we call it the 1st LLM. Its symmetry is opposite to that of the ILM. At the 251kHz transition, another 1st LLM softens and disappears so that only one LLM remains. At each transition step from top to bottom, one LLM peak softens and disappears. The direction of the pump frequency, identified by the dashed arrow in Fig. 2(b), indicates that the ILM is step narrowing at each transition as it becomes weaker in amplitude and so the number of LLM decreases at each transition as well.

Softening of the 1st LLM at the bifurcation point, and step narrowing represent regular behavior for an ILM in the saturable nonlinear lattice. [18] Moreover in a regular saturable nonlinear lattice, the LLM softens either as the pump frequency is increased or decreased towards the step transition. The unusual behavior displayed in Fig. 3 is noteworthy because the 1st LLM does not approach $(f-F)\to 0$ when the pump frequency decreases from bottom to top of Fig. 3.

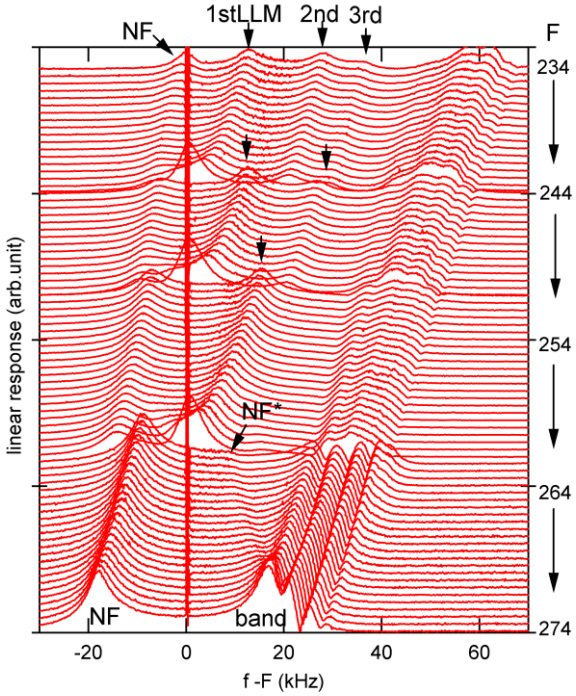

Fig. 3. Linear response spectra for up-scanning the pump frequency. Range from 235.5 to 274kHz as in Fig. 2(b). Spectra are aligned from top to bottom with increasing pump frequency. Abscissa, difference frequency *f-F*, where *F* is pump and *f* is probe frequency. Right ordinate: pump frequency for each spectrum.

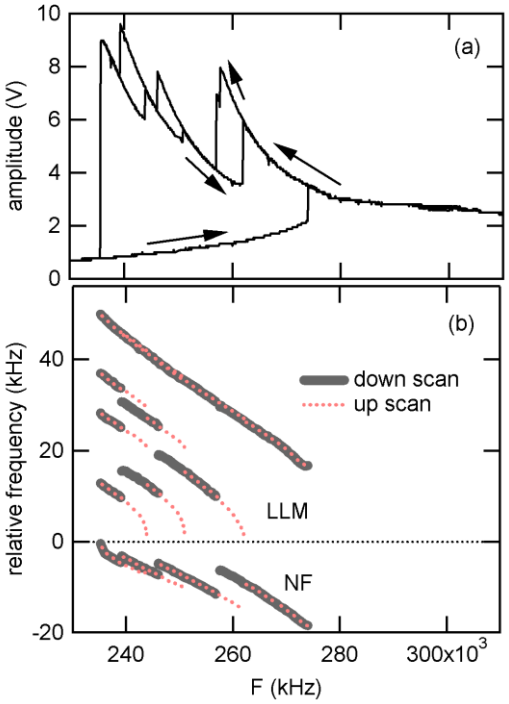

Fig. 4 (a) ILM amplitude as a function of the driver frequency *F*. Both frequency sweep directions are shown by the arrows. The hysteretic signatures are evident. (b) Pump frequency dependences of the NF and the LLMs obtained from linear response spectra.

We also obtained linear response spectra for the down scanning case shown in Fig. 2(a). Figure 4 summarizes these results. The peak amplitude of the ILM in Fig. 2(a) as a function of the pump frequency is presented in Fig. 4(a). The overall structure in the amplitude is similar to that of a Duffing-like response with small saw-tooth changes superimposed. Both of these features display soft nonlinearity and hysteresis. The small hysteretic shifts are produced by step changes in the width of the ILM.

The peak positions of NF, LLM and band edges in Fig. 3 are summarized in Fig. 4(b), with the other measurement for down scanning case shown in Fig. 2(a). The NF shows some steps at these bifurcation points; however, its frequency shift still approaches zero with decreasing pump frequency as expected for a driven-damped system. This is the expected behavior of NF for a Duffing oscillator at a saddle-node bifurcation. The down scanning case corresponds to thick curves in this figure, while red dots are for the up scanning case. Thick curve and dots for each mode overlap in common regions as shown. As described earlier, bifurcation at an up-scanning frequency is signaled by the softening of the 1st LLM. Because there is no softening of the LLMs for the down-scanning case, it is hard to tell what signals the bifurcation in this direction.

4. Conclusions

Because of lattice discreetness and the small size of the lattice used in these experiments we have been able to monitor the quantized behavior of the ILM width in a saturable lattice with increasing or decreasing pump frequency. Hysteresis is observed in these width transitions. Associated with the ILM are LLMs and we used linear spectroscopy to discern the dynamics of these modes at the ILM width transitions. We find that the number of such linear modes changes by one as a transition is crossed. With increasing pump frequency the closest LLM to the ILM shows soft mode behavior at the transition while with decreasing pump frequency the LLM change is abrupt. Either way as the ILM width is increased or decreased at each step one LLM is generated or destroyed. Although these experiments have been carried out on a lattice with only 16 members because the mode is strongly localized the same features are expected to appear for an ILM in a discrete transmission line of any length.

Acknowledgments

M. S. was supported by JSPS-Grant-in-Aid for Scientific Research No. 25400394. A. J. S. was supported by Grant NSF-DMR-0906491.

References

[1] A. J. Sievers and J. B. Page, in *Dynamical Properties of Solids*, edited by G. K. Horton and A. A. Maradudin (North-Holland, Amsterdam, 1995), Vol. 7, p. 137.

[2] D. K. Campbell, S. Flach, and Y. S. Kivshar, Physics Today **57**, 43 (2004).

[3] S. Flach and A. V. Gorbach, Physics Reports **467**, 1 (2008).

[4] S. Flach and C. R. Willis, Physical Review Letters **72**, 1777 (1994).

[5] J. M. Speight and R. S. Ward, Nonlinearity **7**, 475 (1994).

[6] L. Q. English, F. Palmero, A. J. Sievers, P. G. Kevrekidis, and D. H. Barnak, Physical Review E - Statistical, Nonlinear, and Soft Matter Physics **81**, 046605 (2010).

[7] M. Kimura and T. Hikihara, Chaos **19**, 013138 (2009).

[8] Y. Watanabe, K. Hamada, and N. Sugimoto, Journal of the Physical Society of Japan **81**, 014002 (2012).

[9] S. V. Dmitriev, P. G. Kevrekidis, N. Yoshikawa, and D. J. Frantzeskakis, Physical Review E - Statistical, Nonlinear, and Soft Matter Physics **74**, 046609 (2006).

[10] S. Flach, Y. Zolotaryuk, and K. Kladko, Physical Review E - Statistical Physics, Plasmas, Fluids, and Related Interdisciplinary Topics **59**, 6105 (1999).

[11] J. M. Speight, Nonlinearity **10**, 1615 (1997).

[12] Y. Doi and K. Yoshimura, Journal of the Physical Society of Japan **78**, 034401 (2009).

[13] J. Cuevas, J. C. Eilbeck, and N. I. Karachalios, Discrete and Continuous Dynamical Systems **21**, 445 (2008).

[14] L. Hadžievski, A. Maluckov, M. Stepić, and D. Kip, Physical Review Letters **93**, 033901 (2004).

[15] A. Khare, K. Ø. Rasmussen, M. Salerno, M. R. Samuelsen, and A. Saxena, Physical Review E - Statistical, Nonlinear, and Soft Matter Physics **74**, 016607 (2006).

[16] T. R. O. Melvin, A. R. Champneys, P. G. Kevrekidis, and J. Cuevas, Physical Review Letters **97**, 124101 (2006).

[17] M. Syafwan, H. Susanto, S. M. Cox, and B. A. Malomed, Journal of Physics A: Mathematical and Theoretical **45**, 075207 (2012).

[18] W. Shi, S. Shige, Y. Soga, M. Sato, and A. J. Sievers, EPL **103** (2013).

[19] V. Hizhnyakov, A. Shelkan, M. Klopov, S. A. Kiselev, and A. J. Sievers, Physical Review B - Condensed Matter and Materials Physics **73**, 224302 (2006).

[20] M. Sato, S. Imai, N. Fujita, W. Shi, Y. Takao, Y. Sada, B. E. Hubbard, B. Ilic, and A. J. Sievers, Physical Review E - Statistical, Nonlinear, and Soft Matter Physics **87**, 012920 (2013).